PARAMETRIC STUDY OF FLAT SANDWICH MULTILAYER RADOME

A. Kedar and U. K. Revankar

Electronics & Radar Development Establishment
C.V. Raman Nagar, Bangalore-560093, India

Abstract—This paper presents parametric analysis of Flat Sandwich Multilayer Radome using *Boundary Value Solution* technique. The effect of variations in the characteristics of constituent layers of Radome on its microwave transmission properties has been studied. This work has relevance in development of Planar Array Radar Antennas especially for airborne platforms.

1. INTRODUCTION

Radar has to discriminate between the targets and the clutter. In general, the radar cross section (RCS) of the ground is larger than target RCS, and thus calls for a variety of discriminating and filtering techniques [1]. It has been shown that sidelobe level clutter limits the range performance especially for radar mounted on airborne platform, indicating the necessity of ultra low sidelobe level antenna systems. Hence, a Radar Antenna Array protected by a low performance Radome, will be rendered useless, as radome affects the radiation pattern of the array drastically. These effects include, but are not limited to *Boresight Error* and *Boresight Error Slope, Increased Sidelobe Levels, Depolarisation and Insertion Loss* [2].

So far a variety of different approaches [2, 3–5] have been employed to investigate the performance of radome-antenna systems. These approaches can be categorised as: 1) High-frequency methods such as ray-tracing technique, the plane-wave spectrum surface integral technique and Physical Optics method; 2) Low-frequency methods like Method of Moments, FEM and FDTD; and 3) Analytical methods such as dyadic Greens function method and iterative procedures.

For some type of radomes having sharp tips such as ogive or cone shaped, low frequency methods are more accurate but at the cost of extensive computational requirements. However an important
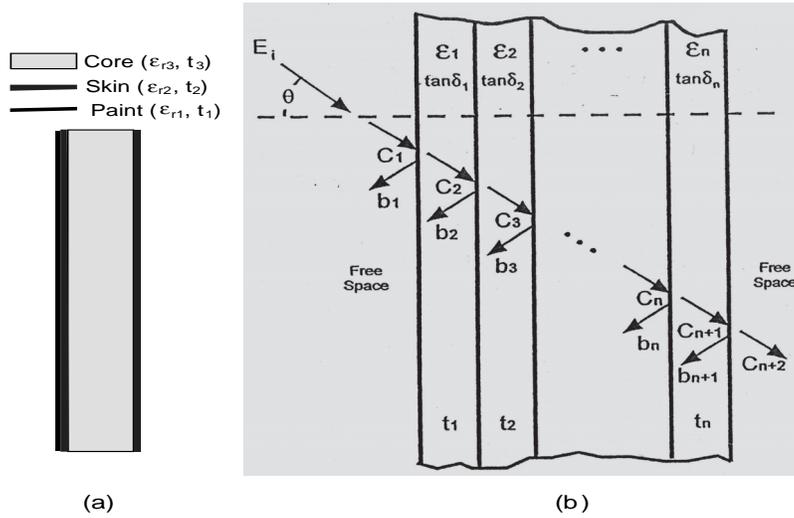
Figure 1. Flat sandwich radome (a). Structure view (b). Boundary-value solution of the N-layer dielectric wall radome.

assumption of high-frequency methods is that the structures have smooth surfaces and electrically large radii of curvature. For most realistic airborne radomes this assumption is most valid. Hence HF method has been employed for analysis in the present work.

Radomes can be classified into various categories as per MIL-R-7705B [6]. In the present study, a *Flat Sandwich Radome* falling under *Style c* [6] has been chosen for the analysis, being suitable for the radar applications on an airborne platform. Flat Sandwich Radome has been analysed using Boundary Value Solution Technique for its performance in S-Band. The effect of the variations in the characteristics of constituent layers of radome, on the microwave transmission performance of radome has been studied. This analysis is expected to be useful in qualifying a radome to be used in various RAA especially for radars applications on airborne platforms.

2. THEORETICAL MODELLING OF FLAT SANDWICH RADOME

The Flat Sandwich Radome Structure [Fig. 1(a)], can be modelled as a *multilayer dielectric* of the N-layer dielectric wall for forward and reverse propagating waves (C_i and B_i, respectively) [Fig. 1(b)]. The

solution takes the following form [2]:

$$\left[\begin{array}{c} C_1 \\ B_1 \end{array} \right] = \prod_{i=1}^{N} \frac{1}{T_i T_{N-1}} \left[\begin{array}{cc} e^{j\gamma_i t_i} & R_i e^{-j\gamma_i t_i} \\ R_i e^{j\gamma_i t_i} & e^{-j\gamma_i t_i} \end{array} \right] \left[\begin{array}{cc} 1 & R_{N+1} \\ R_{N+1} & 1 \end{array} \right] \left[\begin{array}{c} C_{N+1} \\ B_{N+1} \end{array} \right]$$

(1)

In (1), t_i is the Layer thickness of the ith layer; R_i and T_i are Fresnel reflection and transmission coefficients respectively, of the ith layer free space; and γ_i is the propagation constant in the ith layer. The propagation constants can be expressed in terms of angle of incidence relative to the radome normal, θ, as $\gamma_i = k_0 \sqrt{\varepsilon_{ri} - \sin^2 \theta}$, where ε_{ri} is the relative permittivity of the ith layer (a complex quantity), and k_0 is the free space wave number. The Fresnel reflection and transmission coefficients of the ith layer are derivable from the layers' wave impedances, Z_i, through the following expressions:

$$R_i = \frac{Z_i - Z_{i-1}}{Z_i + Z_{i-1}}; \quad T_i = 1 - R_i$$

(2)

In the analysis, polarisations of the incident EM wave front have to be accounted for, by evaluating wave impedances for perpendicular (PER, perpendicular to the plane of incidence) and parallel (PAR, parallel to the plane of incidence) polarisations individually. For the two cases, Z_i is defined as,

$$Z_i = \frac{\cos \theta}{\sqrt{\varepsilon_{ri} - \sin^2 \theta}} \text{ for PER polarisation}$$

(3)

$$Z_i = \frac{\sqrt{\varepsilon_{ri} - \sin^2 \theta}}{\varepsilon_{ri} \cos \theta} \text{ for PAR polarisation}$$

The dielectric loss is modified as $\varepsilon_{ri} = \varepsilon'_{ri} (1 - j \tan \delta_i)$, where ε'_{ri} is the real part of relative permittivity for the ith layer, to consider the dielectric loss. After carrying out multiplications suggested in (1), the result can be written as:

$$\left[\begin{array}{c} C_1 \\ B_1 \end{array} \right] = \left[\begin{array}{cc} A_{11} & A_{12} \\ A_{21} & A_{22} \end{array} \right] \left[\begin{array}{c} C_{N+2} \\ B_{N+2} \end{array} \right]$$

(4)

Radome Efficiency is measurable from the following expression:

$$T_w = |T_w| \angle \text{IPD}; \quad |T_w| = \left. \frac{C_{N+2}}{C_1} \right|_{(B_{N+2}=0)} = \frac{1}{A_{11}}$$

(5)

$|T_w|$ is the *Transmission Coefficient* and *IPD* is the *Insertion Phase Delay*. $|T_w|$ in dB gives the value of *IL* introduced by radome. *IPD*

can be used in estimating depolarisation, BSE, BSES and degradation in SLL due to phase perturbations introduced in the array factor. Radome designers specify the RE in terms of *Radome Transmission Efficiency (RTE)* defined as $|T_w|^2$.

3. PARAMETRIC STUDY OF RADOME

A *Flat Sandwich Radome*, with *Honeycomb Core* [$\varepsilon_{r3} = 1.16$; $t_3 = 1000$ mils (25 mm) typically] and *Fiberglass Epoxy Lamination* [$\varepsilon_{r2} = 4.25$; $t_2 = 33$ mils (0.84 mm) typically] on either side of the honeycomb core along with a *Paint layer* [$\varepsilon_{r1} = 3.65$; $t_1 = 5$ mils (5 mm) typically] has been considered [Fig. 1(a)].

At higher angles of incidence of plane wave on radome surface, to estimate the performance of the radome precisely, average values of RTE and IPD for perpendicular as well as parallel polarisations have to be considered, necessitating the analysis for both the polarisations. Further, effect of variation in dielectric constant and thickness of each constituent layer of flat sandwich radome, on the microwave transmission performance of the flat sandwich radome has been studied. Mainly, core layer should affect RTE and IPD considerably, but lamination and paint layers, both are having high dielectric constants and their combined thickness is nearly 1 mm. Therefore, any variation in thickness and/or in the dielectric constant of these layers will affect the flat sandwich radome performance considerably. Considering the fact, effect of variation in characteristics of lamination and paint layers on the flat sandwich radome performance can not be ignored and has to be studied.

The response curves of RTE and IPD (i) w.r.t. frequency of operation, f; (ii) w.r.t. angle of incidence of plane wave on radome surface; (iii) w.r.t. thickness of core; and (iv) w.r.t. thickness and dielectric constant of lamination and paint layers have been studied and discussed in the following sub-sections.

3.1. RTE and IPD vs. Frequency of Operation

The variation in RTE and IPD w.r.t. frequency of operation, f, being varied from DC to 7 GHz has been studied and plotted [Fig. 2 and Fig. 3]. This study has been carried out at angle of incidence; $0°$ (normal incidence) and $60°$, for parallel as well as perpendicular Polarisations and the observations have been summarised in Table 1. For angle of incidence, $0°$, response curves for RTE and IPD w.r.t. f, have coincided for both the parallel and perpendicular polarisations, as expected [Fig. 2 and Fig. 3]. The magnitude of RTE remains above

98% and IPD varies by $\pm 1.5°$ (max.) over 15% bandwidth around centre frequency $(f_0 = 3.3\,\text{GHz})$ as is evident from Table 1, [see Fig. 2 and Fig. 3].

Table 1. Variation of RTE and IPD with respect to frequency at $0°$ and $60°$ angles of incidence.

Angle of Incidence of Plane Wave (¡)	RTE (%) (Over 15% BW)		IPD (¡) (Over 15% BW)	
	PER	PAR	PER	PAR
0	> 98	> 98	± 1.5	± 1.5
60	88.2 ± 1	98.2 ± 0.2	± 2.0	± 1.7

The magnitude of RTE at f_0 is 88.2% and 98.2% at angle of incidence, $60°$, for perpendicular and PAR Polarisations, respectively, [Fig. 2 and Table 1]. RTE varies by $\pm 1\%$ (max.) for perpendicular polarisation and by $\pm 0.2\%$ (max.) for PAR Polarisation over 15% bandwidth around, f_0, [Fig. 2 and Table 1]. Further, it has been observed that IPD varies by $\pm 2°$ (max.) for perpendicular polarisation and $\pm 1.7°$ (max.) for PAR Polarisation over 15% BW around, f_0 [Fig. 3 and Table 1]. Although with the increase in frequency, RTE and IPD have been found to be deteriorating, but it can be concluded from the Table 1 and Figures 2 and 3, that within S-band, flat sandwich radome performs in conformation to MIL-R-7705B [6].

3.2. RTE and IPD vs. Angle of Incidence

The variation in RTE and IPD, w.r.t. angle of incidence for perpendicular and parallel polarisations at $f_0 + 6.5\%\ f_0$ has been shown in Fig. 4 and Fig. 5. The observations have been summarised in Table 2. The magnitude of RTE has been observed above 89% w.r.t. variation in angle of incidence up to $60°$, but afterwards it degrades rapidly [Fig. 4 and Table 2] for the perpendicular polarisation. For parallel polarisation, the magnitude of RTE remains above the specified magnitude [6] even beyond $60°$, with slow degradation rate of RTE w.r.t. angle of incidence [Table 2].

It has been observed that IPD varies by $1.07°$, $3.65°$ and $8.72°$ in the respective sectors of angle of incidence; $0°$ to $20°$, $21°$ to $40°$ and $41°$ to $60°$, for perpendicular polarisation [Fig. 5 and Table 2]. Whereas, for parallel polarisation the variation in IPD is $0.04°$, $0.85°$ and $4.19°$ in the respective sectors of angle of incidence; $0°$ to $20°$, $21°$ to $40°$ and 41 to $60°$, [Fig. 5 and Table 2]. It can be inferred that the variation in IPD is very gradual up to $60°$, but beyond $60°$ it
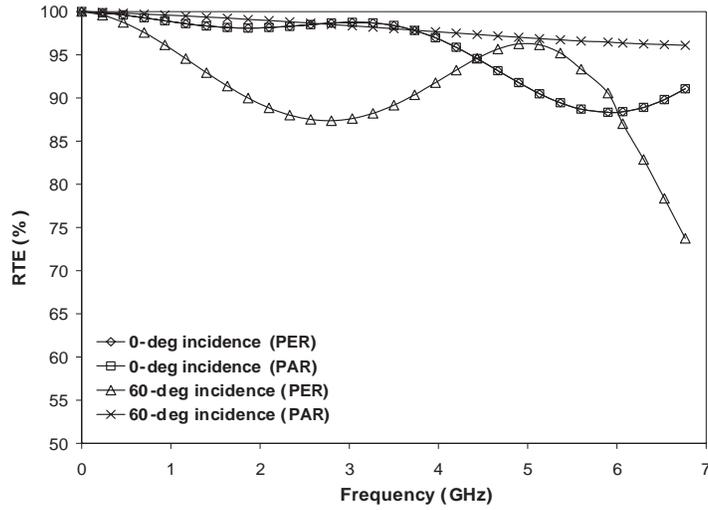
Figure 2. Response curves for RTE w.r.t. frequency at angles of incidence, 0° and 60°, for perpendicular (PER) and parallel (PAR) polarisations.
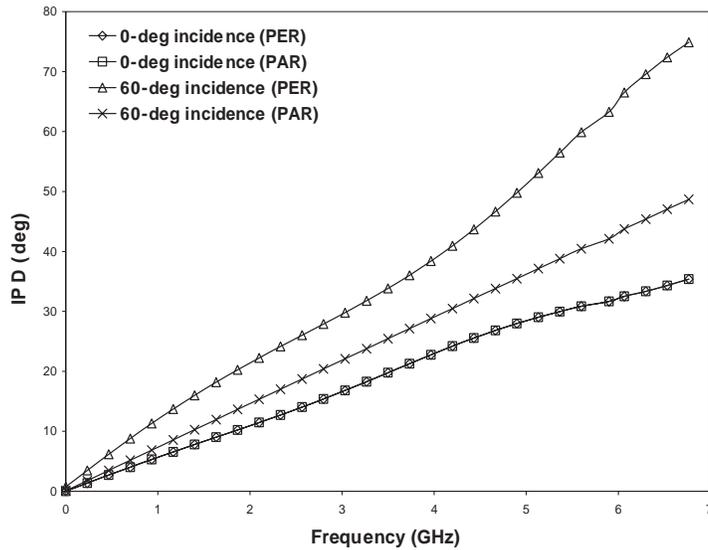
Figure 3. Response curves for IPD w.r.t. frequency at angles of incidence, 0° and 60°, for perpendicular (PER) and parallel (PAR) polarisations.
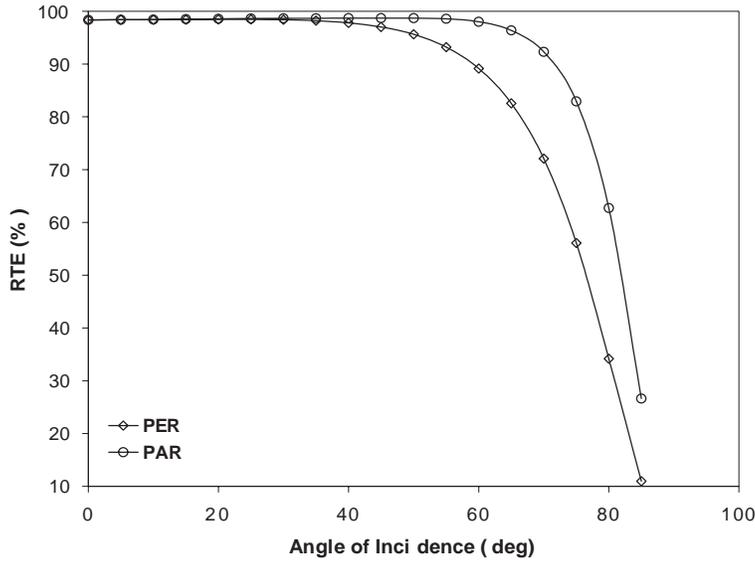
Figure 4. Response curves for RTE w.r.t. angle of incidence for perpendicular (PER) and parallel (PAR) polarisations at the operating frequency, $f_0 + 6.5\%\ f_0$.
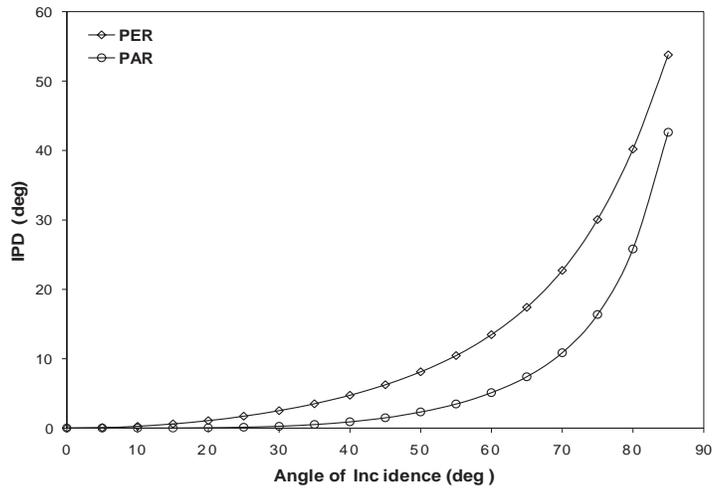
Figure 5. Response curves for IPD w.r.t. angle of incidence for perpendicular (PER) and parallel (PAR) polarisations at the operating frequency, $f_0 + 6.5\%\ f_0$.

Table 2. Variation of RTE and IPD with respect to angle of incidence.

Angle of Incidence of Plane wave (¡)	RTE (%)		IPD variation (¡)	
	PER	PAR	PER	PAR
0-20	>98.4	>98.56	0 to 1.0721 (~1.07¡ variation)	0 to 0.038 (~0.04¡ variation)
21-40	>97.8	>98.69	1.0721 to 4.7302 (~3.65¡ variation)	0.038 to 0.8944 (~0.85¡ variation)
41-60	>89.1	>98.01	4.7302 to 13.4547 (~ 8.72¡ variation)	0.8944 to 5.0873 (~4.19¡ variation)

varies appreciably in large amounts. The variation is more in case of perpendicular polarisation as compared to parallel polarisation.

3.3. RTE and IPD vs. Core of Radome

The variation of RTE and IPD with respect to variation in core thickness, t_3 (= 25 mm) of radome, varied in range of ± 5 mm around t_3, at angle of incidence, $0°$ and $60°$, at $f_0 + 6.5\%$ f_0, [Fig. 6 and Fig. 7]. The results have been summarised in Table 3. The variation in magnitude of RTE and IPD is same at angle of incidence, $0°$ for both parallel as well as perpendicular polarisations as shown in Table 3 and Figures 6 and 7. The variation in RTE is 1.3% (max.) over the complete range 25 ± 5 mm. The value of RTE is above 97% over the complete range for parallel and perpendicular polarisations at $0°$ incidence [Fig. 6 and Table 3], which is acceptable as per ref. [6]. At angle of incidence, $60°$, the magnitude of RTE varies by 0.4% (max.) for parallel polarisation and 4% (max.) for perpendicular polarisations [Fig. 6 and Table 3]. The magnitude of RTE remains above 88% and 97% in case of perpendicular and parallel polarisations, respectively, acceptable as per ref. [6].

At angle of incidence, $0°$, variation in IPD over the range 25 ± 5 mm is $4°$ (max.) for parallel as well as perpendicular polarisations [Fig. 7 and Table 3]. Further, it has been observed that within ± 2 mm variation in the core thickness the variation is only $\pm 0.83°$ (max.) [Fig. 7 and Table 3]. Further, the variation in IPD with t_3 over complete range is $6°$ to $7°$, at $60°$ incidence. But, within ± 2 mm variation in t_3, IPD varies by only $\pm 1.2°$ (max.). Thus the electrical performance of radome can be maintained within tolerable limits as per the MIL-R-7705B [6] for ± 2 mm variation in the thickness of the core material of radome.
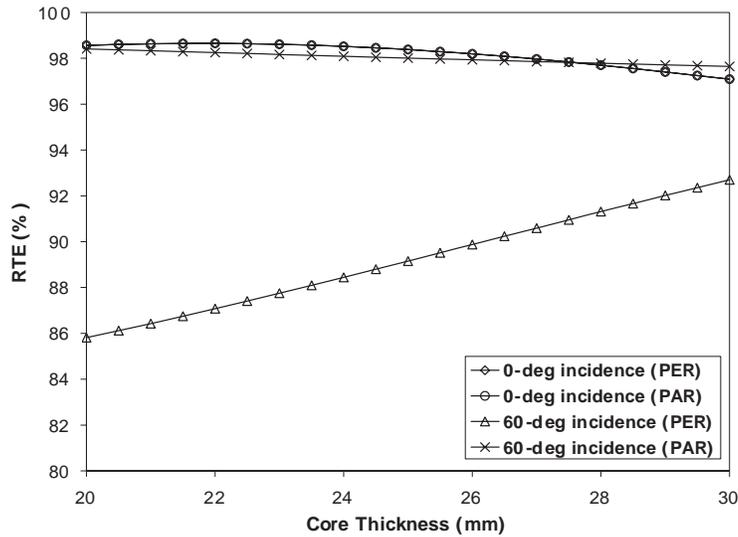
Figure 6. Response curves for IPD w.r.t. core thickness at angles of incidence, 0° and 60°, for perpendicular (PER) and parallel (PAR) polarisations at the operating frequency, $f_0 + 6.5\% \ f_0$.
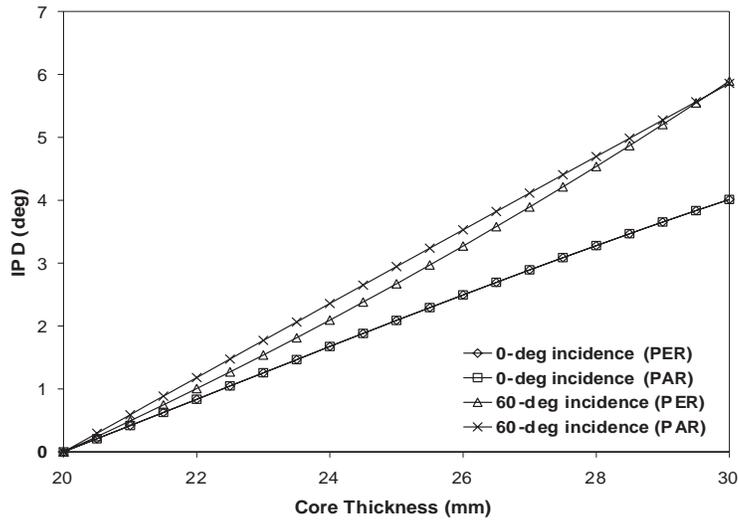
Figure 7. Response curves IPD w.r.t. core thickness at angles of incidence, 0° and 60°, for perpendicular (PER) and parallel (PAR) polarisations at the operating frequency, $f_0 + 6.5\% \ f_0$.

Table 3. Variation of RTE and IPD with respect to core thickness of radome at 0°- and 60°-angles of incidence.

Angle of Incidence of Plane wave (¡)	Variation in Thickness (w.r.t. 25mm core) (mm)	RTE (%)		IPD variation (¡)	
		PER	PAR	PER	PAR
0	± 5	>97	>97	± 2	± 2
0	± 2	>98	>98	± 0.81	± 0.81
60	± 5	85-92	>97	± 2.94	± 2.94
60	± 2	88-90	>97.8	± 1.17	± 1.17

3.4. RTE and IPD vs. Variation in Characteristics of Lamination or Skin Layer

The Lamination ($\varepsilon_{r2} = 4.25$) of thickness $0.84\,\text{mm}$ ($t_2 = 33\,\text{mils}$) is existing on both sides of the core of radome. In the analysis, maximum variation of 10% (worst case) has been considered in ε_{r2} and t_2 of lamination. The effect of variation in ε_{r2} and t_2 on either side (towards antenna array or towards free space) and on the both sides of the core has been considered on RTE and IPD, [Tables 4 and 5]. The analysis has been carried out at $f_0 + 6.5\%\ f_0$.

Table 4. Variation in RTE and IPD w.r.t. variation (by ±10%) in thickness of lamination or skin layer of radome.

Variation in t_2 (thickness of Lamination or Skin Layer) by ± 10%	Angle of Incidence of Plane Wave Radome surface (°)	RTE (%)		IPD (°)	
		PER	PAR	PER	PAR
Towards antenna surface	0	0.1	0.1	1.11	1.11
	60	0.22	0.04	1.5	0.95
Towards free space	0	0.16	0.16	1.09	1.09
	60	0.415	0.055	1.5	0.95
On both sides of radome core	0	0.257	0.257	2.21	2.21
	60	0.592	0.088	3	1.89

3.4.1. Effect of Variation in Thickness

Table 4 shows the variation of RTE and IPD when the t_2 is varied from 29.7 mils to 36.3 mils, i.e., $\pm 5\%$ around 33.0 mils, for the three cases, i.e., towards antenna surface; towards free space; and on both sides of the core layer for perpendicular as well as parallel polarisations at 0° and 60° incidences.

It can be clearly inferred from the Table 4 that variation in t_2 on either side does not have much effect on RTE and IPD for angle of incidence, 0°, but, it has considerable effect at angle of incidence, 60°. Further, when variation in t_2 is considered on both sides of the core, considerable variation has been observed in the RTE and IPD even at angle of incidence, 0°.

3.4.2. Effect of Variation in Dielectric Constant, ε_{r2}

Table 5 shows the variation in RTE and IPD with respect to variation in the ε_{r2}, when it is varied from 3.825 to 4.675, i.e., $\pm 5\%$ around ε_{r2} (= 4.25), for the three cases, i.e., towards antenna surface; towards free space; and on both sides of the radome core (The sign, $\uparrow$, shows that value of RTE/IPD increases from lower to higher side, whereas, it is decreasing, by default, in all the cases.

Table 5. Variation in RTE and IPD w.r.t. variation (by $\pm 10\%$) in dielectric constant of lamination or skin layer of radome.

Variation in ε_{r2} (dielectric constant of Lamination or Skin Layer) by ± 10%	Angle of Incidence of Plane Wave Radome surface (°)	RTE (%)		IPD (°)	
		PER	PAR	PER	PAR
Towards antenna surface	0	0.08	0.08	1.42	1.42
	60	0.31	0.012($\uparrow$)	1.91	0.87
Towards free space	0	0.162	0.162	1.38	1.38
	60	0.47	0.008($\uparrow$)	1.88	0.85
On both sides of radome core	0	0.26	0.26	2.8	2.8
	60	0.8828	0.021($\uparrow$)	3.79	1.72

Again it can be inferred from the Table 5 that any variation in ε_{r2} for perpendicular polarisation case or for angle of incidence, 60°, there is a considerable variation in RTE and IPD. Further, when the

variation in ε_{r2} is considered on both sides of the radome core there is a considerable variation in RTE and IPD even at angle of incidence, $0°$, or for parallel polarisation.

3.5. RTE and IPD vs. Variation in Characteristics of Paint Layer

The paint layer is a thin layer [$\varepsilon_{r1} = 3.65$; $t_1 = 5\,\text{mil}$] existing over the lamination to protect radome from the environmental hazards. In the analysis, maximum variation of $\pm 1\%$ (worst case) has been considered in ε_{r1} and t_3 from the fabrication point of view. Table 6 shows the variation in RTE and IPD w.r.t. variation in ε_{r1} and t_3 for perpendicular and parallel polarisations at $0°$ and $60°$, angles of incidence. The analysis has been carried out at $f_0 + 6.5\%$ f_0. It has been observed that the variation in dielectric constant and thickness of paint layer does not affect the performance of the radome considerably [Table 6].

Table 6. Variation in RTE and IPD w.r.t. variation (by $\pm 5\%$) in thickness and dielectric constant of plaint layer of radome.

Variation in characteristics of Paint Layer of Radome by ± 5%	Angle of Incidence of Plane Wave Radome surface (°)	RTE (%)		IPD (°)	
		PER	PAR	PER	PAR
In Thickness	0	0.002	0.002	0.01	0.01
	60	0.005	0.001	0.01	0.009
In Dielectric Constant	0	0.003	0.003	0.02	0.02
	60	0.007	0.0006	0.02	0.01

4. CONCLUSION

In the presented work, it has been shown that while assessing a radome for its usage in particular Radar Antenna Array, its tolerance analysis w.r.t variation in characteristics of all of its constituent layers has to be carried out. This is necessary for defining manufacturing tolerances on fabrication of radome so that it can qualify to be used in various radar antenna systems with an airborne platform and other radar applications.

In the study, the effect of the variation in the characteristics of the constituent layers of radome on the microwave transmission properties of radome has been discussed. It has been shown that variations in all the constituent layers may affect the radome performance considerably and hence have to be constrained within tolerable limits. This work finds useful application in qualifying a radome for radar antenna systems with an airborne platform and other radar applications.

ACKNOWLEDGMENT

REFERENCES

1. Williams, F. C. and M. E. Radant, "Airborne radars and the three PRFs," *Microwave Journal*, 129–135, 1983.
2. Kozakoff, D. J., *Analysis of Radome-Enclosed Antennas*, Artech House, 1997.
3. Li, L.-W., L. Zhou, M. S. Leong, T.-S. Yeo, and P. S. Kooi, "An open-ended circular waveguide with an infinite conducting flange covered by a dielectric hemi-spherical radome shell: Full-wave analysis and Green Dyadics," *Progress In Electromagnetics Research*, PIER 21, 221–245, 1999.
4. Li, L.-W. and W.-X. Zhang, "Electromagnetic scattering of a thin circular loop enclosed by a spherical chiral radome shell: A method of moments analysis," *Progress In Electromagnetics Research*, PIER 35, 141–163, 2002.
5. Nie, X.-C., N. Yuan, L.-W. Li, T.-S. Yeo, and Y.-B. Gan, "Fast analysis of electromagnetic transmission through arbitrary shaped airborne radomes using precorrected-FFT method," *Progress In Electromagnetics Research*, PIER 54, 37–59, 2005.
6. Military Specifications Radomes General Specifications For, MIL-R-7705B, 1988.